



## Coupling of a bimetallic strip heat engine with a piezoelectric transducer for thermal energy harvesting

J. Boughaleb, A. Arnaud, S. Monfray, P.J. Cottinet, S. Quenard, F. Boeuf, D. Guyomar & T. Skotnicki

To cite this article: J. Boughaleb, A. Arnaud, S. Monfray, P.J. Cottinet, S. Quenard, F. Boeuf, D. Guyomar & T. Skotnicki (2016) Coupling of a bimetallic strip heat engine with a piezoelectric transducer for thermal energy harvesting, *Molecular Crystals and Liquid Crystals*, 628:1, 15-22, DOI: [10.1080/15421406.2015.1137390](https://doi.org/10.1080/15421406.2015.1137390)

To link to this article: <http://dx.doi.org/10.1080/15421406.2015.1137390>



Published online: 13 May 2016.



Submit your article to this journal [↗](#)



Article views: 33



View related articles [↗](#)



View Crossmark data [↗](#)

# Coupling of a bimetallic strip heat engine with a piezoelectric transducer for thermal energy harvesting

J. Boughaleb<sup>a,b,c</sup>, A. Arnaud<sup>a</sup>, S. Monfray<sup>a</sup>, P.J. Cottinet<sup>b</sup>, S. Quenard<sup>c</sup>, F. Boeuf<sup>a</sup>,  
D. Guyomar<sup>b</sup>, and T. Skotnicki<sup>a</sup>

<sup>a</sup>STMicroelectronics, SAS, Crolles Cedex, France; <sup>b</sup>LGEF, INSA Lyon, Villeurbanne Cedex, France; <sup>c</sup>CEA Liten, Grenoble Cedex 9, France

## ABSTRACT

The field of energy harvesting became attractive due to the development of wireless sensors networks. Consequently many systems emerged to harvest wasted energies to convert it into usable electrical energy. The goal behind these harvesters is to be able to supply low power sensor nodes. The research work described in this paper deals with a thermal energy harvester based on a double stage conversion to obtain usable electrical energy. More specifically, this paper presents the properties of the materials used in this harvester. It concerns its components, its thermal modeling and optimization, its electrical modeling and finally the piezoelectric benchmark.

## KEYWORDS

energy harvesting;  
piezoelectric transducer;  
bimetallic strip heat engine;  
material properties

## 1. Introduction

Energy harvesting is attracting more and more researchers due to the abundant kinds of wasted energies in our environment that could be harvested. But this is not the only reason; it now catches more attention because of the development of wireless sensor networks that raises the problem of power supply [1–2]. Many fields can be attracted by these wireless networks such as environmental or industrial control, health monitoring and so on. Usually supplied by batteries, these systems raise the problem of their short lifetime and the necessary wiring. Alternatives to batteries have then been developed and are based on energy harvesting system. These can be of many kinds, using for example solar energy with photovoltaic modules, thermal energy thanks to pyroelectric materials and thermoelectric structures, or even mechanical energy using piezoelectric structures.

The study presented in this paper deals with the specificities of our harvester in many domains. In fact, the harvester presented first by Skotnicki in [3] has previously been studied from an electrical point of view [4–8], from a thermal point of view too [9], but until now no paper has focused on its materials specificities and how all the studies realized until now are linked due to the interactions between the materials choices, the structure's design etc. In this research paper, we focus consequently all our attention on the materials specificities and their role to increase the performances.

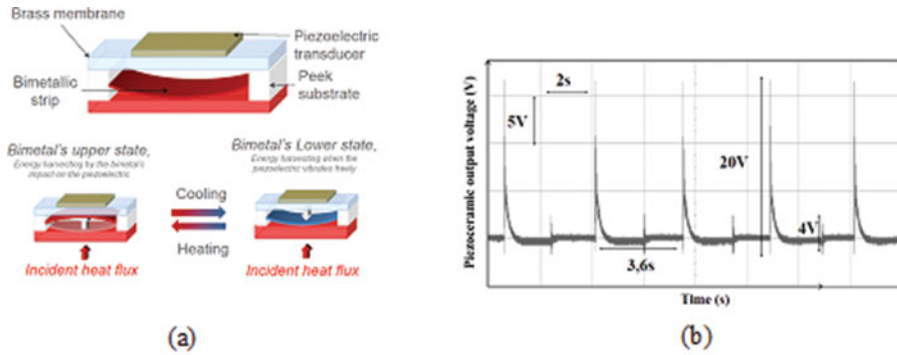


**Figure 1.** (a) Scheme of the coupled piezoelectric–bimetal heat engine with the upper state of the bimetal and its lower state, (b) output signal of that harvester.

## 2. Working principle of the heat engine

### 2.1. A double transduction for thermal energy harvesting

The thermal energy harvester we have conceived is based on a double step conversion mechanism. First, heat is absorbed by the bimetal until the thermal bending moments achieve a threshold value which makes it snap; this is the thermo-mechanical energy conversion. When the bimetal has snapped, it is at its upper position and it is being cooled down by the cold surface without any radiator or heat sink. Exactly the same way as before, bending moments in the opposite direction are created and once a threshold value is achieved, the bimetal snaps down. This is the explanation of the whole bimetal cycling during the first conversion mechanism. The second step of this conversion allowing the creation of electrical charges is the one insured by a piezoelectric membrane. This membrane is impacted or released each time the bimetal respectively snaps up or down. This functioning of the complete device is illustrated in Fig. 1. The two phases when electrical energy is generated are shown, as well as the different components of the harvester and the output signal.

### 2.2. Bimetal working principle and piezoelectric transduction

The heat engines we use in our harvesters are a shell-like bimetals made from two materials with different and opposite thermal properties: Invar (Fe-Ni 36%) acting as the low coefficient of thermal expansion (CTE) layer and NC4 (Fe-Ni 22%-Cr 3%) acting as the high CTE layer. This way, the bimetal realizes the conversion of thermal energy into kinetic energy [8] (Fig. 2a).

However, to understand how the bimetal works, it is important to understand the reasons of its thermo-mechanical bi-stability. As said previously, the bimetals are made of two material layers having different coefficients of thermal expansion. This difference makes them curve when they are exposed to a certain temperature but it is not enough to create a thermo-mechanical bi-stability [10]. In addition to this first aspect, and as explained by Wittrick in the case of bimetallic shells [11], by combining this CTE mismatch with another property having an antagonistic effect (like an initial curvature), a mechanical bi-stability is observed. For our bimetals, the two aspects are combined to have thermic bi-stable bimetals that release their kinetic energy at each snap up or down. All these explanations are represented on Fig. 2b that clearly shows the consequence of each aspect separately and the result of the combination of both.

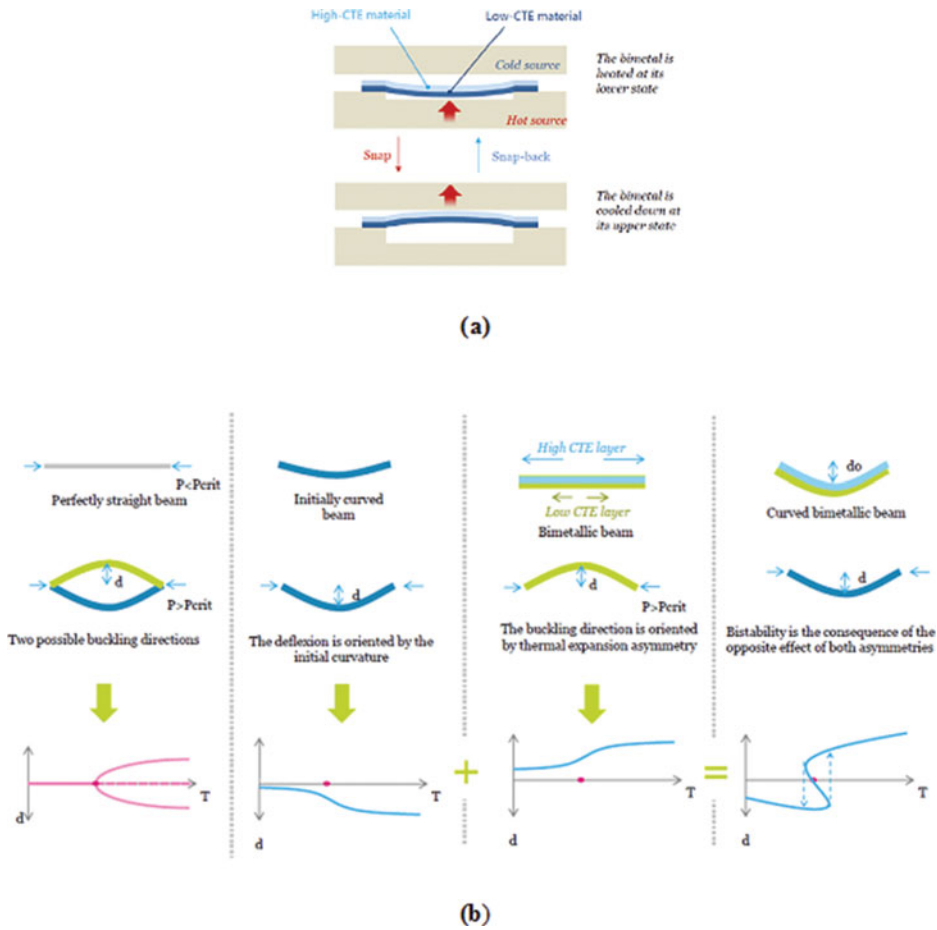


**Figure 2.** Working principle of the thermal energy harvester with the bimetal cycling (a) and explanation of the bimetals buckling principle (b).

### 3. Thermal optimization and its effects on the electrical specificities

The harvesters we are currently presenting in this paper have been widely studied [4–8] but no thermal investigation has been done on it to improve its performances thermally and consequently electrically. For this reason, we established a thermal model to understand all the means by which heat is transferred in the structure and also to know exactly the temperature difference across the harvester between the hot source and the cold surface (because the bimetal oscillates between those two sources). The model is exposed in [9] and experimental measurements carried out on the harvester for a range of hot source temperature going from 40°C to 100°C are shown in Fig. 3. The analytical model for the temperature difference across the harvester is in a good agreement with the experimental measurements. In this first harvester, the substrate is in PTFE (Teflon) that has good thermal specificities (its thermal conductivity was about 0,23 W/K<sup>-1</sup>M<sup>-1</sup>) but degrades mechanical ones as its young modulus was equal to 300MPa. Consequently, the piezo clamping was not very rigid and the quality factor measured on the electrical signals did not exceed 7, and the maximum output voltage reached was about 10V in the best case.

To improve the thermal properties, we used the model referred previously and we designed a bigger air cavity inside the structure and changed the substrate material by a better one for

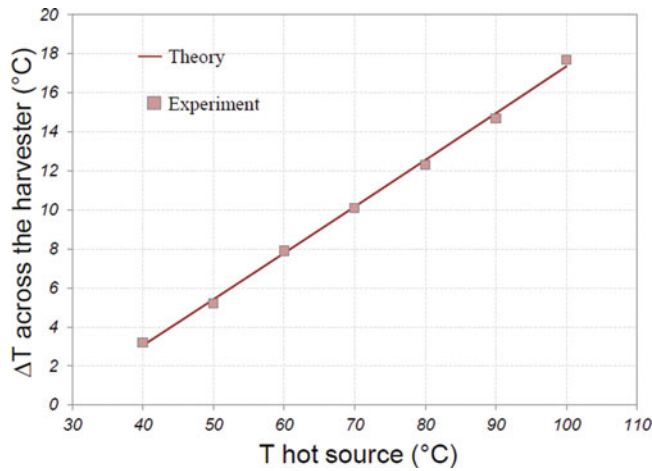


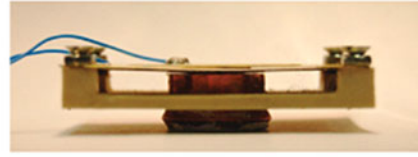
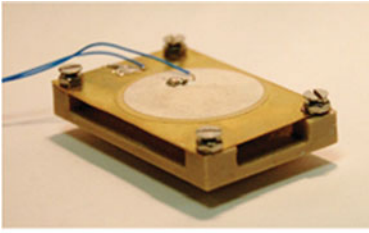
**Figure 3.** Thermal difference across the harvester before the thermal improvements.

our use cases. This material is the PEEK that has a low thermal conductivity  $0.25 \text{ W/K}^{-1}\text{M}^{-1}$  but the mechanical properties are much better: the PEEK's young modulus is equal to 4GPa which makes the piezo clamping much more rigid. This implies directly a better energy harvesting because less mechanical energy will be lost in the clamp as shown in Fig. 4a. Moreover, combining the new material choice with the improved harvester design explained in [9], the thermal specificities were improved: the temperature difference across the harvester was two times higher (Fig. 4b); then the electrical properties were improved from  $2\mu\text{W}$  maximum with the non-optimized system, we managed to obtain  $32 \mu\text{w}$  per bimetal which is a huge advancement for the optimized process.

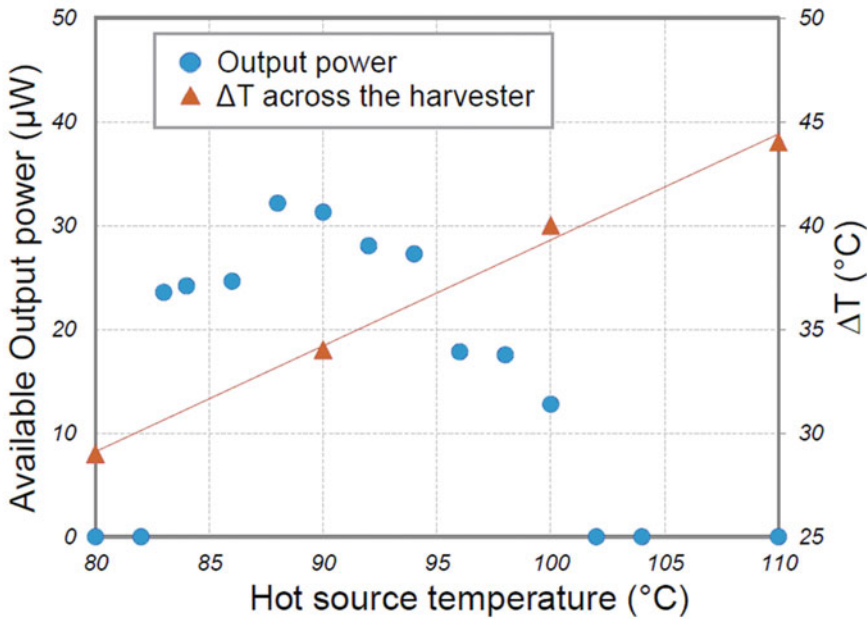
Another important point achieved by the thermal optimization is that for each bimetal having a fixed snapping temperature and a fixed snapping back temperature, (for example a bimetal  $67^\circ\text{C}/70^\circ\text{C}$ ) it could only oscillate on a reduced hot range temperature around its thermal equilibrium (a maximum of  $\pm 3^\circ\text{C}$ ) with the non-optimized design. Now, with the optimized structure, the same bimetal can keep on snapping on a hot range of hot source temperature of  $19^\circ\text{C}$  as shown on Fig. 4b.

#### 4. Electrical modeling of the piezoelectric and bimetal interaction by a lumped element model

An electrical model of the entire harvester was needed to be able to simulate the real signals provided by the harvester when the bimetal oscillates. Consequently, a spice model based on the lumped element model of a piezoelectric transducer with voltage sources representing the bimetal's action is established based on Mason's model of the piezoelectric oscillators [12]. Knowing that the piezo membrane and the bimetal have two equilibrium states and that the mechanical parameters depend strongly on the boundary conditions, in the circuit Fig. 5a, an electrical branch is modeled for the piezo capacitance and the probe value and two mechanical branches are used: the first one represents the system when the bimetal is at its upper state and the second one when the bimetal is at its lower state. First of all, in this model, L shown as an inductor represents the inertial term, C represents the stiffness term and finally R is the damping and the mechanical losses. Depending on the bimetal state, the values of these parameters are completely different: when the bimetal is at the upper position, the total



(a)



(b)

**Figure 4.** Device new design after the thermal optimization (a) and effect of the thermal optimization on the electrical properties (b).

Vibrating mass is much more important than the case when it is down which explains  $L_{up} > L_{down}$ . Following the same reasoning, the mechanical losses are more important when the bimetal is at its upper state which explains  $R_{up} > R_{down}$ . Concerning the system's stiffness, the value is nearly the same in the two cases because its value depends on the whole structure and not just the bimetal and the piezoelectric.

Concerning the voltage sources that represent the bimetal's impact on the piezoceramic, two different cases are modeled: when the bimetal is up, a square-wave signal represents the impacts on the piezoelement because the bimetal keeps in contact with the cold surface until its temperature reaches the snapping back temperature. In the other case, when the bimetal snaps back, it is more modeled as a Dirac impulse because it releases very quickly the piezo membrane that can vibrate freely (Fig. 5b).

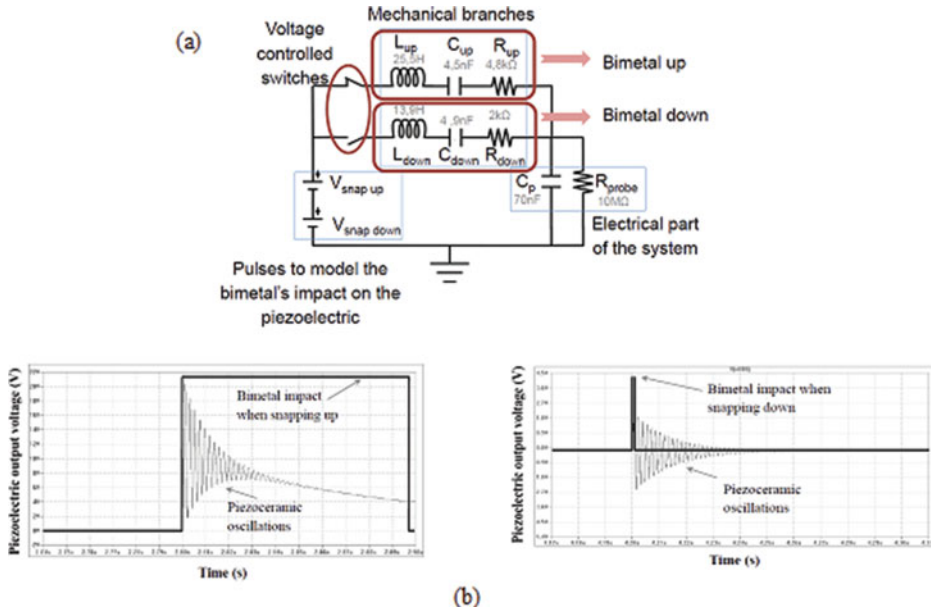


**Figure 5.** (a) SPICE electromechanical modeling of the harvester, (b) simulation of the bimetal snaps up and down.

As shown on the Fig. 5b, each voltage peak is a damped oscillatory signal  $V(t)$ , so the energy is extracted using (1) and the power using (2) where ( $Q$  is the signal's quality factor,  $\omega$  the signal's pulsation,  $C_p$  the piezoelectric capacitance and  $V_0$  the signal's voltage first pic amplitude) and the power  $P$  using equation (2) (where  $f$  is the cycling frequency of the bimetal). We obtain  $32\mu W$  of available electrical power using these formulas.

$$E_p = C_p \cdot \omega \int_{t_1}^{t_2} |v(t)|^2 dt = \frac{V_0^2 \cdot Q(4 \cdot Q^2 + 2)}{2 \cdot \omega(4 \cdot Q^2 + 1)} \cdot C_p \cdot \omega \quad (1)$$

$$P = E_p \cdot f \quad (2)$$

## 5. Piezoelectric study and benchmarking

The constitutive equations of piezoelectricity are written in (3) and (4)

$$\delta = \frac{\sigma}{Y} + dE \quad (3)$$

$$D = \varepsilon E + d\sigma \quad (4)$$

Where  $D$  is the charge density,  $E$  the electric field,  $d$  the piezoelectric strain constant,  $\sigma$  the mechanical stress,  $Y$  is the young modulus and  $\varepsilon$  the dielectric constant of the piezoelectric material. We use our piezomembrane in the 31 mode because the system is much more compliant and consequently, smaller input forces can produce larger strains. The aim of this part is to present the benchmark done to choose the best piezoelectric material for energy harvesting from our supplier. To do so, we used the same methodology as the one used in [13]. This paper has played a key role in our study as it showed the influence of each piezoelectric parameter on the output power comparing all kinds of piezo-materials: single crystal, PVDF, hard PZT and soft PZT.

Data from Table 1 are extracted from paper [13] and the main results of this study is that combining the Factor Of Merit (FOM) with the  $d_{31}$  parameter is recommended to choose a

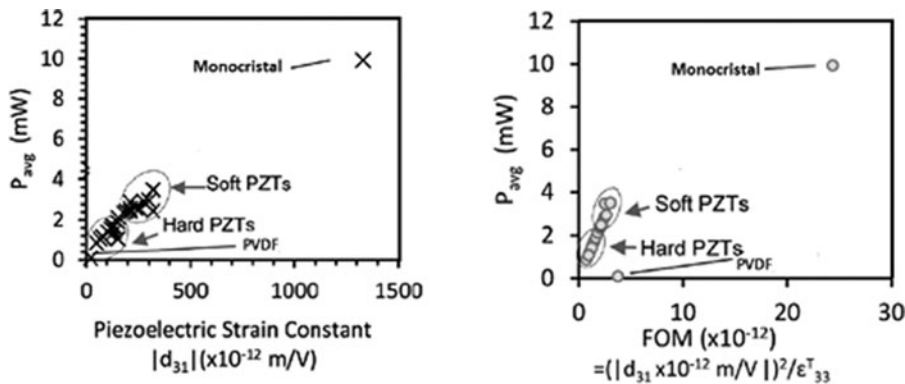


**Table 1.** Piezoelectric materials proprieties and calculation of the factor of merit FOM.

Material parameter	properties	unit	KP-PZT-4 4M11	KP-PZT-4D 4M13	KP-PZT-8 8M10	KP-PZT-5A 5M18
K31	constant	$10^{-12}\text{C/N}$	0,3	0,33	0,31	0,35
d31			−140	−150	−100	−172
$\varepsilon_{33}/\varepsilon_0$	dielectric constant		1200	1400	1030	1800
Tc	curie temperature	°C	330	320	300	358
FOM		$10^{-24}$	16,3	16,1	9,71	16,4
d31	curie temperature	$10^{-12}\text{C/N}$	140	150	100	172
Tc			330	320	300	358

KP-PZT-5B 5M20	KP-PZT-5B 5M23	KP-PZT-5B 5M25	KP-PZT-5T 5M27	KP-PZT-5T 5M27D	KP-PZT-5H 5H32	KP-PZT-5H 5H38	KP-PZT- 5×5H45
0,36	0,37	0,33	0,38	0,39	0,39	0,38	0,36
−186	−230	−200	−230	−210	−275	−280	−350
2000	2350	2500	2700	2750	3200	3800	4300
316	290	292	280	280	260	250	178
17,3	22,5	16	19,6	16,0	23,6	20,6	28,5
186	230	200	230	210	275	280	350
316	290	292	280	280	260	250	178



**Figure 6.** Effect of the  $d_{31}$  and the FOM on the output power of piezoelectric generators [13].

material for piezoelectric energy harvesting. It was in fact shown first, as we see in Fig. 6a, that  $d_{31}$  is a more dominant parameter than the others for higher output voltages. Secondly, FOM was more linearly related to the output power (Fig. 6b). Thus, we used this strategy to compare all the available materials we have in table (1) knowing that:

$$FOM = d^2/\varepsilon$$

From this study, and knowing that our harvester is a thermal energy harvesting, the operating temperature is an important factor to take into account. We found two materials having the highest factor of merit but whose curie's temperatures are different. Knowing that we aim at using our energy harvester in temperature range going from 40°C to 200°C, the KP-PZT-5H 5H32 whose Tc is 260°C seems more adapted to higher temperatures and the KP-PZT-5×5H45 whose Tc is 178°C has a higher FOM than the previous material and can be used for lower temperatures and will be experimented in the future.



## 6. Conclusion and outlooks

This paper presents a thermal energy harvester based on a two steps conversion mechanism from a new point a view. Contrary to the previous papers in which this device was studied and presented, we focus here on the material properties of the whole structure, we explained how the different improvements were investigated whether it is from a thermal point of view, a mechanical one or even in relation with the piezoelectric materials. This gives a global view of the current structure and explains its functioning in details once the materials properties are well known and the choices of each component is justified. Finally, in the last part, a new piezoelectric material seems to be very promising for the future applications at low temperatures (lower than 150°C) as its FOM is the highest of all the piezomaterials our supplier designs.

## Acknowledgments

This work was co-funded by the Fonds Unique Interministériel (FUI), through the HEATec project.

## References

- [1] Steingart, D. (2009). Power sources for wireless sensor networks. In: Priya, S. and Inman, D. J. (Ed.), *Energy harvesting technologies*, Springer, New York, NY, p. 269.
- [2] Merrett, G. W. *et al.* (2010). Wireless devices and sensor networks, In: Beeby, S. and White, N. (Ed.), Norwood, Atech House, Chapter 2, p. 9.
- [3] Skotnicki, T. (2009). Dispositifs de conversion d'énergie thermique en électricité, *French Patent*, FR2951873 (A1).
- [4] Puscasu, O. *et al.* (2012). An innovative heat harvesting technology (HEATec) for above-Seebeck performance. *IEEE International Electron Devices Meeting*, (San Francisco, CA, 10-13 Dec. 2012), pp. 12.5.1-12.5.4.
- [5] Boisseau, S. *et al.* (2013). Semi-flexible bimetal-based thermal energy harvesters. *Smart Mater. Struct.*, 22.
- [6] Puscasu, O. *et al.* (2014). *Sensor Actuat a-phys A*, 214, 7–14.
- [7] Boughaleb, J. *et al.* (2014). Spice modeling of a coupled piezoelectric–bimetal heat engine for autonomous wireless sensor nodes power supply. *Proc. PowerMEMS*, (Japan, Awaji Island, 18-21 November 2014), pp. 457–461.
- [8] Arnaud, A. *et al.* (2013). Piezoelectric and electrostatic bimetal-based thermal energy harvesters. *Proc. PowerMEMS*, (London, UK, 3-6 December 2013), pp. 295–299.
- [9] Boughaleb, J. *et al.* Thermal modeling and optimization of a thermally-matched energy harvester. Submitted to Smart Materials and Structures.
- [10] Arnaud, A. *et al.* (2014). Modeling of the thermo-mechanical efficiency of the bimetalstrip heat engines. *Proc. PowerMEMS*, (Japan, Awaji Island, 18-21 November 2014), 85–89.
- [11] Wittrick, W. H. *et al.* (1953). Stability of a bimetallic disk. *Q J Mechanics Appl Math*, 6, 15–31.
- [12] Mason, W. P. (1935). Proc. of the Institute of Radio Engineers. *IEEE*, 23, 1252–1263.
- [13] Daniels, A. *et al.* (2013). *IEEE*, 60(12), 2626–2633.